Water Research, Volume 130, 1 March 2018, pp. 20-30
DOI:10.1016/j.watres.2017.11.049

# The role of algal organic matter in the separation of algae and cyanobacteria using the novel "Posi" - dissolved air flotation process

Narasinga Rao Hanumanth Rao,[1,2] Russell Yap,[1,3] Michael Whittaker,[2,4] Richard M. Stuetz,[1,5] Bruce Jefferson,[6] William L. Peirson,[7] Anthony M. Granville,[2,8] and Rita K. Henderson,[1,*]

[1] bioMASS Lab, School of Chemical Engineering, The University of New South Wales, Sydney NSW 2052, Australia.

[2] Centre for Advanced Macromolecular Design, School of Chemical Engineering, The University of New South Wales, Sydney NSW 2052, Australia.

[3] BASF Corp. Charlotte, North Carolina 28273, USA (Current address)

[4] ARC Centre of Excellence in Convergent Bio-Nano Science and Technology, Monash Institute of Pharmaceutical Sciences, Monash University – Parkville Campus, VIC 3052, Australia (current address).

[5] UNSW Water Research Centre, School of Civil and Environmental Engineering, The University of New South Wales, Sydney NSW 2052, Australia.

[6] Cranfield Water Science Institute, School of Applied Sciences, Cranfield University, Bedfordshire, MK43 0AL, UK.

[7] Water Research Laboratory, School of Civil and Environmental Engineering, The University of New South Wales, Manly Vale NSW 2093, Australia.

[8] TDK Research Solutions, Bondi Junction, NSW 2022, Australia (current address)

* Corresponding author: r.henderson@unsw.edu.au

**ABSTRACT**

Algae and cyanobacteria frequently require separation from liquid media in both water treatment and algae culturing for biotechnology applications. The effectiveness of cell separation using a novel dissolved air flotation process that incorporates positively charged bubbles (PosiDAF) has recently been of interest but has been shown to be dependent on the algae or cyanobacteria species tested. Previously, it was hypothesised that algal organic matter (AOM) could be impacting the separation efficiency. Hence, this study investigates the influence of AOM on cell separation using PosiDAF, in which bubbles are modified using a commercially available cationic polyelectrolyte poly(N, N-diallyl-N,N-dimethylammonium chloride) (PDADMAC). The separation of *Chlorella vulgaris* CS-42/7, *Mychonastes homosphaera* CS-556/01 and two strains of *Microcystis aeruginosa* (CS-564/01 and CS-555/1), all of which have similar cell morphology but different AOM character, was investigated. By testing the cell separation in the presence and absence of AOM, it was determined that AOM enhanced cell separation for all the strains but to different extents depending on the quantity and composition of carbohydrates and proteins in the AOM. By extracting AOM from the strain for which optimal separation was observed and adding it to the others, cell separation improved from <55% to >90%. This was attributed to elevated levels of acidic carbohydrates as well as glycoprotein-carbohydrate conjugations, which in turn were related to the nature and quantity of proteins and carbohydrates present in the AOM. Therefore, it was concluded that process optimisation requires an in-depth understanding of the AOM and its components. If culturing algae for biotechnology applications, this indicates that strain selection is not only important with respect to high value product content, but also for cell separation.

**Keywords:** Algae harvesting, cyanobacteria, dissolved air flotation, polymer coated bubbles

## 1. INTRODUCTION

Algal cells are separated in applications that involve both water treatment and algae harvesting for biotechnology (Bernhardt *et al.* 1991, Pieterse *et al.* 1997, Kempeneers *et al.* 2001, Anthony *et al.* 2013, Weschler *et al.* 2013). Dissolved air flotation (DAF) is often applied to separate the cells by the addition of chemicals such as coagulants and flocculants that selectively vary particle character (Henderson *et al.* 2008a, Edzwald 2010, Coward *et al.* 2013). Recently, the surface modification of microbubbles generated in DAF via polymer addition to the saturator has received attention as an alternative to traditional coagulation-flocculation of influent particles in the fields of water treatment for natural organic matter removal (Malley 1995, Han *et al.* 2006, Shi *et al.* 2017), algal separation and harvesting (Henderson *et al.* 2008c, Henderson *et al.* 2009, Henderson *et al.* 2010b, Yap *et al.* 2014), and mineral processing (Oliveira *et al.* 2012). In the field of algal separation and harvesting, the modified bubble DAF process also known as PosiDAF, has great potential for algae cell separation (Henderson *et al.* 2009), particularly because of benefits such as reduced chemical demand, removal of metal-salt contamination from the float and reduction in sludge volume, and an increased solid-liquid ratio of the float (Henderson *et al.* 2009).

However, while greater than 95% separation has been achieved for certain algae and cyanobacteria in PosiDAF (Henderson *et al.* 2010b, Yap *et al.* 2014), cell separation and float characteristics were observed to vary depending on species and strain despite morphological similarity. For example, it was found that cell separation efficiencies for UK strains of *Microcystis aeruginosa* and the green algae *Chlorella vulgaris* were 96% and 74%, respectively, despite both having similar morphology (Henderson *et al.* 2010b). Additionally, for most species, cell removal was greater than that predicted by the theoretical white water model, attributed to differences in AOM character (Henderson *et al.* 2010b). In a further study, (Yap *et al.* 2014) achieved 99% cell removal of the cyanobacteria *M. aeruginosa* CS-

564/01, observing that fibrous web-like ‘strands’ formed that enhanced flotation, although further investigation was not undertaken into their nature. Given the morphological similarities of the cells in the aforementioned examples, this variability was thus attributed to differences in the composition of algal organic matter (AOM) between the species.

Typically, AOM comprises hydrophilic polysaccharides, hydrophobic proteins and other low molecular weight soluble microbial products (Henderson *et al.* 2008b, Pivokonsky *et al.* 2014, Pivokonsky *et al.* 2016). Over a range of studies, AOM has been shown to both hinder and enhance conventional coagulation and flocculation of algae (Bernhardt *et al.* 1985, Pivokonsky *et al.* 2006, Takaara *et al.* 2007, Henderson *et al.* 2010b). For example Bernhardt *et al.* (1985), demonstrated that low concentrations of AOM can behave as a flocculant aid for *Dictyosphaerium*; however, higher concentrations inhibited flocculation. More recently, (Pivokonsky *et al.* 2006) and (Takaara *et al.* 2007) showed that the proteins present in the AOM from *M. aeruginosa* could decrease coagulation efficiency by preferentially complexing with coagulants.

Several techniques such as total and dissolved organic carbon (Henderson *et al.* 2008b, Fang *et al.* 2010), specific ultraviolet absorption (SUVA) (Henderson *et al.* 2008b, Pivokonsky *et al.* 2014), protein and polysaccharide concentration measurements (Henderson *et al.* 2008b, Pivokonsky *et al.* 2014), charge measurements (Henderson *et al.* 2008b, Henderson *et al.* 2010a), advanced techniques such as gravimetric determination or mass spectrometry (Dubois *et al.* 1956, Lin 2007), size exclusion chromatography (SEC) (Henderson *et al.* 2008b, Zhang *et al.* 2013), fluorescence spectroscopy (Henderson *et al.* 2008b, Fang *et al.* 2010, Qu *et al.* 2012) and Fourier transform infrared (FT-IR) spectroscopy (Giordano *et al.* 2001, Murdock *et al.* 2009, Chon *et al.* 2013) have previously been used to characterise AOM and its components. However, no studies have investigated the link between PosiDAF performance and the variability in AOM composition.

Hence, the aim of this study was to improve the understanding of how AOM influences algal and cyanobacterial cell separation in the PosiDAF process. To achieve this, comparisons of the PosiDAF jar test performance between *C. vulgaris* (strain CS-42/7), *M. homosphaera* (strain CS-556/01) and two strains of *M. aeruginosa* (CS-555/1 and CS-564/01), which were known to be of comparable morphology but very different AOM composition, were undertaken and related to the AOM character including the composition of resulting fibrous networks. Furthermore, experiments examining the influence of extracted AOM when dosed stepwise into the jars were conducted. Overall, this paper establishes that the presence of AOM and its biochemical character can be directly related to the effectiveness of the PosiDAF process.

## 2. MATERIALS AND METHODS

### 2.1 Chemicals

Low molecular weight PDADMAC (Sigma Aldrich, Australia) was used for PosiDAF jar testing. To prepare the background sample matrix, sodium chloride (Ajax Finechem, Australia) and sodium bicarbonate (Ajax Finechem, Australia) were made into 1.0 and 0.1 M solutions with Milli-Q water for jar testing. To adjust the pH, 1M hydrochloric acid (HCl) (Ajax Finechem, Australia) and 1M sodium hydroxide (NaOH) solutions (Ajax Finechem, Australia) were used.. Alcian blue 8GX powder (Sigma-Aldrich, Australia) was dissolved in 3% acetic acid solution prior to use as a stain for charged polysaccharides. A solution of 8% paraformaldehyde (PFA) (ProSci Tech, Australia) was used as a fixation agent to prevent possible biochemical changes that could occur while drying samples for Fourier transform infrared spectroscopy analysis.

## 2.2 Algae and cyanobacteria

*C. vulgaris* CS-4/7, *M. homosphaera* CS-556/01 and two strains of *M. aeruginosa*, CS-555/1 and CS-564/01, known hereafter as CV, MH, MA555 and MA564, respectively, were obtained from the Commonwealth Scientific and Industrial Research Organisation's (CSIRO) Australian National Algae Culture Collection (ANACC) (Hobart, Australia) and recultured in Jaworski and MLA media (Bolch *et al.* 1996, Henderson *et al.* 2010b). Cultures were grown and stored based on methods described previously (Yap *et al.* 2014).

## 2.3 Algal organic matter extraction

The AOM was separated from the cells to produce three AOM solutions. First, cells were separated from AOM by centrifugation at 10,000 x g for 15 minutes with an Allegra® X-15R Centrifuge (Beckman Coulter, Australia) (Henderson *et al.* 2008b). To remove any additional tightly-bound AOM, each aliquot of pelleted cells was resuspended in their respective media without micronutrients by vortexing for 20 seconds, followed by another cycle of centrifugation. The supernatants from the centrifuge cycles were collected and combined to give $AOM_C$. An aliquot of this supernatant ($AOM_C$) was then filtered using 934-AH glass microfiber filters (1.50 µm nominal pore size, Whatman, USA) to remove cell debris to give $AOM_{1.50}$. The size of AOM molecules has previously been implicated in process performance (Henderson *et al.* 2010a) and, hence, a further aliquot of the $AOM_{1.50}$ solution was then filtered using a 0.45 µm polyethersulphone (PES) syringe filter, resulting in $AOM_{0.45}$, thus enabling investigation of the impact of AOM size on PosiDAF performance.

## 2.4 Algal system characterisation

### *2.4.1 Cell properties*

A haemocytometer and light microscope (DM500, Leica Microsystems Ltd, Switzerland) were used for cell counting. The cell size measurements were made using a Mastersizer 2000 (Malvern, UK). Cultures were adjusted to pH 7 with 1 M HCl for charge analysis which was undertaken using two techniques: zeta potential measurements were conducted with a Zetasizer Nano ZS (Malvern, UK) and charge demand analyses with a PCD-04 Particle Charge Detector (Mütek BTG, Switzerland). Each analytical procedure was conducted in triplicate.

### *2.4.2 Analysis of AOM*

The three AOM solutions ($AOM_C$, $AOM_{1.50}$ and $AOM_{0.45}$) were analysed with a TOC–Vsch Analyser (Shimadzu, Australia) to determine their concentration as total organic carbon (TOC). Protein and carbohydrate assays were conducted using the modified Lowry method with bovine serum albumin as standard (Frølund *et al.* 1995) and phenol-sulphuric acid method with D-glucose as standard (Zhang *et al.* 1999), respectively. Each measurement was conducted in triplicate.

$AOM_{0.45}$ was further analysed using size exclusion liquid chromatography with organic carbon and $UV_{254}$ (LC-OCD Model 8) (DOC Labor, Germany). A Toyopearl TSK HW-50S column was used that has a particle size of 30 mm, length of 250 mm and internal diameter of 20 mm. The mobile phase employed was phosphate buffer at pH 6.37 (2.5 $g \cdot L^{-1}$ $KH_2PO_4$ and 1.5 $g \cdot L^{-1}$ $Na_2(HPO_4)_2 \cdot H_2O$) at a flow rate of 1.1 $mL \cdot min^{-1}$. An injection volume of 1 mL was used to analyse the samples. From this analysis, the apparent molecular weight of molecules within the $AOM_{0.45}$ with respect to DOC and UV absorbing compounds was analysed (Huber

*et al.* 2011). Note that it was not possible to analyse $AOM_C$ or $AOM_{1.50}$ as the chromatographic column is protected by an in-line 0.45 µm filter.

Charge measurements were conducted on the three AOM samples corrected to pH 7 with 1 M HCl. Zeta potential measurements were conducted with a Zetasizer Nano ZS (Malvern, UK) and charge demand analysis with a PCD-04 Particle Charge Detector (Mütek BTG, Switzerland). Each measurement was conducted in triplicate.

In order to detect and quantify the acidic carbohydrates in the AOM, Alcian blue staining was performed on samples collected during the onset of the stationary phase of cell growth, based on the procedure outlined in previous studies (Passow *et al.* 1995, Villacorte *et al.* 2015a, Villacorte *et al.* 2015b). Briefly, the cultures were filtered using 0.45 µm polycarbonate membrane and stained with Alcian Blue at pH of 2.5. The staining was performed at pH 2.5 to ensure that both sulphated and carboxylated polysaccharides were detectable (Passow *et al.* 1995). Images of the stained acidic carbohydrates were obtained through a light microscope (DM2500, Leica Microsystems Ltd, Switzerland) and processed with *Image J* software. The acidic carbohydrates were quantified from the image by selecting random areas of 0.18 $mm^2$.

## 2.5 Jar Test Procedures

### *2.5.1 PosiDAF jar tests*

PosiDAF jar testing of CV, MH, MA555 and MA 564 was carried out using PDADMAC as described in previous studies (Henderson *et al.* 2010b, Yap *et al.* 2014). As with conventional DAF jar testing, PosiDAF jar tester and saturator solutions were prepared using Milli-Q water (18.2 MΩ·cm) with 0.5 mM $NaHCO_3$ and brought to an ionic concentration of 1.8 mM using NaCl. The cells were added to the jar tester solution to give a concentration of $7.5 \times 10^5$

cells·mL$^{-1}$. A recycle ratio of 20% was selected for all tests, with a saturator pressure of 450 kPa and a flotation time of 10 minutes, ensuring a high bubble to particle ratio.

*2.5.2 Investigation of the influence of AOM on PosiDAF performance*

PosiDAF jar tests as described in section 2.5.1 were repeated by fixing the PDADMAC dose at the point where maximum cell removal was observed for the respective species. However, in these experiments, the AOM concentration was varied by first separating AOM from the cells (according to the method outlined in section 2.3) and resuspending cells in buffer solution to the appropriate concentration, and then reintroducing AOM into the cell systems with mixing at 50 rpm for 60 seconds to the desired AOM concentration.

*Experiment 1:*

Strains of CV, MH, MA555 and MA564 with the AOM removed as described in 2.3 were used to prepare jar test samples of 7.5 $\times 10^5$ cells·mL$^{-1}$. Jar tests were first performed in the absence of AOM. Subsequently, the $AOM_C$ obtained from the strain under investigation was reintroduced to prepare cell solutions with AOM concentrations ranging from 0.25 to 2.0 mg·L$^{-1}$.

*Experiment 2:*

The strains for which poor separation was observed during Experiment 1 were used to provide cell cultures for the jar test; however, the AOM obtained from the strain for which the best separation was observed was introduced. This determined whether the separation could be improved upon by the addition of "foreign" AOM. Similar to Experiment 1, $AOM_C$ was reintroduced to prepare concentrations ranging from 0.25 to 2.6 mg·L$^{-1}$. This time, the same tests with $AOM_C$ were repeated using $AOM_{1.50}$ and $AOM_{0.45}$ over the same dosing range to determine whether AOM size impacted treatability.

*Experiment 3:*

The strain for which poorest separation was observed during Experiment 1 was used to provide cell cultures for the jar test and $AOM_{1.50}$ from the strain for which the best separation was observed was introduced. However, these experiments were conducted for different sub-cultures of the best performing strain over a period of one year to test the repeatability of the experiments from Experiment 2.

*2.5.3 Analysis of flotation performance*

Analysis of jar test performance included cell counting using a haemocytometer or Sedgewick Rafter to determine residual cyanobacteria cell concentration (Henderson *et al.* 2010b). Zeta potential analysis was performed using a Zetasizer Nano ZS (Malvern, UK). All measurements were undertaken in triplicate.

*2.5.4 Fourier transform infrared spectroscopy (FT-IR) imaging analysis*

The fibrous 'strands' from the AOM of *M. aeruginosa* CS-564/01, that were previously described by (Yap *et al.* 2014) as flotation enhancers, were again observed in this study during PosiDAF jar tests; however, in this case they were analysed by FT-IR imaging following the procedure used by Gonzalez-Torres *et al.* (2017). Briefly, the strands were extracted from the jars during PosiDAF experiments and fixed using the PFA. The fixed samples were then transferred to a stainless steel slide, dried and analysed by FT-IR imaging using a PerkinElmer Spotlight 400 FT-IR microscope (USA). FT-IR images were collected over the 4000-750 $cm^{-1}$ using reflectance mode and chemi-maps were created from the FT-IR image files in specific ranges using *Spectrum* software. The chemi-maps created for the proteins, acidic carbohydrates and carbohydrates were overlaid to obtain the FT-IR images. These macromolecules were selected as they have previously been implicated to have an

influence on cell separation (Mopper *et al.* 1995, Henderson *et al.* 2010a, Villacorte *et al.* 2015b, Pivokonsky *et al.* 2016). The spectra were also extracted and plotted by *Microsoft Excel* (Version 2013) to obtain the cross-section profiles.

## 3 RESULTS

### 3.1 Algal system characterisation

The CV, MH, MA564 and MA555 cells had similar spherical, unicellular morphology when grown in the laboratory. The physical diameter of the spherical cells of CV was found to be bigger (5±0.6 µm) than those of MA555 (3.0±0.7 µm), MA564 (3.1±0.6 µm) and MH (2.8 ±0.5 µm) (Table 1A). The sizes of MA555 and MA564 were almost 40% lower than that observed for *M. aeruginosa* (CCAP 1450/3) that was used in a previous PosiDAF study (Henderson *et al.* 2010b) while that of CV was almost 1.5 times the size of the strain used in the same study.

The cultures were also found to have widely differing charge; for instance, while MA555 had the least negative zeta potential (-17.0±1.0 mV) and charge density ($-9.3\times10^{-7}$ meq·cell$^{-1}$), MA564 and MH had highly negative zeta potentials (approximately -35 mV) and charge (approximately $-15\times10^{-7}$ meq·cell$^{-1}$) (Table 1A). Similar trends were seen in the zeta potential of the AOM fractions of the cultures (Table 1A). Interestingly, the charge density and zeta potential of the AOM fractions became less negative for every fraction with the most negative values for $AOM_C$ and the least negative for $AOM_{0.45}$. The lower negative charge observed for the $AOM_{0.45}$ fractions when compared to the other fractions in all the species points to the presence and high concentration of low molecular weight charged compounds. Collectively, the disparities in charge and size of the algal cell suspension indicate that the relative dose per cell for all the species could fluctuate for the same polyelectrolyte concentration.

$AOM_C$ extracted from strain MA564 had greater than two to three times the TOC concentration in comparison to that from MH, CV and MA555. Conversely, the DOC of the extract ($AOM_{0.45}$) was found to be slightly more concentrated for MA555 at $9.6\times10^{-10}$ mg·cell$^{-1}$ than that observed for the others (Table 1B). When the biopolymer composition was analysed, it was noticed that all fractions of MA564 AOM had the highest total protein and carbohydrate concentration, and at least twice as much protein:DOC and thrice as much carbohydrate:DOC ratios than the AOM from other strains (Table 1B). However, the protein:DOC and carbohydrate:DOC ratios between the $AOM_{0.45}$ and $AOM_{1.50}$ fractions from every strain were very similar. The carbohydrate:DOC ratio of MA555 (0.38 mg·mg$^{-1}$) was also similar to that of the UK strain of MA; however, the protein:DOC ratio of the UK strain was found to be much greater than that for the strains used in this current paper at 0.64 mg·mg$^{-1}$ (Table 1B). With $AOM_C$, it was revealed that the protein:TOC and carbohydrate:TOC ratios were much lower than the $AOM_{0.45}$ and $AOM_{1.50}$ fractions. For example, in Table 1B, it is seen that MA564 had a protein:TOC ratio of 0.11±0.02 mg·mg$^{-1}$ while that of the $AOM_{1.50}$ was 0.26±0.06 mg·mg$^{-1}$. This may due to the fact that cell debris was not effectively removed by centrifugation in $AOM_C$, increasing observed TOC concentrations. Collectively, it can be said that the overall concentrations of biopolymers were found to be present in the greatest quantity in the AOM from MA564.

An LC-OCD analysis of $AOM_{0.45}$ from the strains used in this study revealed some differences in the size fractions of the AOM from the different strains (Table S1, Figure S1). Specifically, MA564 had a larger fraction of biopolymers, humic substances and building blocks at 18.5%, 14.7% and 45%, respectively, in comparison to MA555, MH and CV. In contrast, the LMW neutrals fractions were the lowest for MA564 (21%) compared to MA555 (31%), MH (45%) and CV (23%), respectively (Table S1, Figure S1). These results

demonstrate a tendency for higher molecular weight components to exist in the MA564 AOM.

When Alcian Blue was used to stain acidic carbohydrates (SI Figure S2), aggregates of these molecules were visible under a microscope for all the species indicating that they were produced extracellularly during the onset of the stationary phase and not just via release due to the death of algal cells or environmental stress as observed previously (Passow 2002, Villacorte *et al.* 2015a, Villacorte *et al.* 2015b). However, the concentrations were species dependent; with MA564 producing more than five times the acidic carbohydrate concentration at a surface coverage of 52% of polycarbonate membrane than MH (Table 1B). This is further supported by the fact that the AOM from MA564 had at least three times or higher carbohydrate concentrations when compared to the other species at the same time period (Table 1B, Figure S5). However, the presence of acidic carbohydrates was not reflected when comparing the carbohydrate concentrations of $AOM_{0.45}$ and $AOM_{1.50}$ fractions. For instance, the carbohydrate concentrations of MA564 $AOM_{1.50}$ and $AOM_{0.45}$ were 8 $mg \cdot L^{-1}$ and 7.5 $mg \cdot L^{-1}$, respectively (Figure S5). With the acidic carbohydrates likely to be filtered out by the 0.45 µm membrane, it is expected that the carbohydrate concentrations of the $AOM_{0.45}$ fractions would be lower than the $AOM_{1.50}$ fractions; however, comparable values were observed for all the species (Figure S5).

(Table 1A and 1B)

**3.2 PosiDAF Jar Tests**

When applying PosiDAF using PDADMAC, the zeta potential of the treated effluents became positive at doses above 0.001 $meq \cdot L^{-1}$for MA555, 0.002 $meq \cdot L^{-1}$ for MA564, and approximately 0.008 $meq \cdot L^{-1}$ for CV and MH (Figure 1). Despite belonging to the same species, a key difference in the effluent zeta potential between MA555 and MA564 was that

the dose required to neutralise charge of MA555 with PDADMAC was one sixth that required for MA564. However, for CV it was noted that the dose required to neutralise charge with PDADMAC was twice as high as that observed for *C. vulgaris* CCAP 211/11B (Henderson *et al.* 2010b).

The PosiDAF cell separation varied for the different species and strains: MA564 and MA555 reached a maximum cell separation of 95±3% and 31±2%, respectively, at a polymer dose of 0.001 meq·$L^{-1}$ while CV and MH reached a maximum of 62±3% and 35±2% at a polymer dose of 0.004 meq·$L^{-1}$ (Figure 1). Above the optimal polymer dose, cell separation decreased for all the strains except MA564. The effective separation of MA564 is in line with previous observations made for *M. aeruginosa* CS-564/01 and CCAP-1450/3, where separations of 96% - 99% were observed [8, 9]. A similar decrease in separation effectiveness to that obtained for *C .vulgaris* CS-42/7 was observed for a UK strain of *C. vulgaris* CCAP 211/11B (Henderson *et al.* 2010b). Given the previously described similarities in morphological characteristics, the discrepancies in cell removal and effluent zeta potential are attributed to AOM influences, interactions of polymers and other high molecular weight substances.

(Figure 1)

### 3.3 Investigating the link between PosiDAF cell separation and AOM composition

#### 3.3.1 FT-IR analysis of web-like strands from MA564

Web-like strands were observed only during the jar tests of MA564. On examination of the FT-IR spectra of these strands (Figure S3), nine regions with peaks that have been previously reported to be those of macromolecules were found (Giordano *et al.* 2001, Mecozzi *et al.* 2001, Sigee *et al.* 2002, Lee *et al.* 2006, Murdock *et al.* 2009, Chon *et al.* 2013, Sudharsan *et al.* 2015) (Table S2). A broad peak around 3300 $cm^{-1}$ in region (1) was attributed to the

presence of hydrogen-bonded OH caused by the hydroxyl groups in carbohydrates as well as residual moisture. The C-H stretch caused by the lipids present in the strands was visible in all the samples (2). Peaks in region 3 were attributed to C=O stretching from aldehydes, ketones and protonated carboxylic acids. The peaks had a poor signal in this region indicative of poor concentration of the aforementioned compounds. Broad peaks in (4) and (5) were indicative of the amide binding protein, amide I (4) and amide II (5). A strong carboxylate anion peak was observed at 1340 $cm^{-1}$ (6). A single peak in the region (7) was attributed to the sulphated esters ($R\text{-}O\text{-}SO_3^-$) present in the samples. However, the signal was not strong and may reflect the limited presence of the sulphated compounds. A group of overlapping peaks (8) and (9) around 1150-1050 $cm^{-1}$ were observed which were the result of a contribution from different types of polysaccharides that have been detected previously in algal species (Villacorte *et al.* 2015b) and speculated to be glycogen molecules that serve as energy storage in the cells (Bertocchi *et al.* 1990, Murdock *et al.* 2009, Hadjoudja *et al.* 2010).

FT-IR images of the spatial distribution of proteins, acidic carbohydrates and carbohydrates for the strand edge and center were obtained as they provided information on the extent of aggregation or homogeneity of these macromolecules across the samples (Figure 2 (B) to (E)). The analysis of the FT-IR images of the strand edge (Figure 2B, C) revealed the presence of regions attributed to proteins (red, amide I peak at 1630 $cm^{-1}$), carbohydrates in Figure 2B (green, C-O vibration at 1030 $cm^{-1}$) and acidic carbohydrates in Figure 2C (green, $COO^-$ vibration at 1330 $cm^{-1}$). The sample in Figure 2C exhibited a more homogeneous distribution of proteins and acidic carbohydrates (yellowish-orange hue) in comparison to the same sample in Figure 2B, which had a more localised distribution and distinctive differences between proteins and carbohydrates. By analysing the corresponding cross-section images of the strand edge (Figure 2B, 2C), it was observed that changes in the red protein line correlate

well with most changes in the green acidic carbohydrate line in Figure 2C, whereas in Figure 2B, the cross-section image shows poor correlation between the red protein line and green carbohydrate line. When the FT-IR images of the strand center (Figure 2D, 2E) were analysed, it was seen that both acidic carbohydrates and carbohydrates had moderate homogeneity in their distribution with the proteins. This phenomenon was also validated by their corresponding cross-section images (Figures 2D, 2E). Overall, it was observed that the yellowish-orange regions of protein-acidic carbohydrate homogeneity dominated more towards the strand edges when compared to the strand center where both the acidic carbohydrates and carbohydrates had moderate influences. The homo- and heterogeneous distribution of proteins with acidic carbohydrates and carbohydrates, respectively, along with the correlations observed between these regions in the cross section images may be caused by the conjugation of glycoproteins and carbohydrates that has been previously observed in algal systems (Kehr *et al.* 2015).

(Figure 2)

### 3.3.2 Cell separation as a function of acidic carbohydrate concentration

On investigating the link between maximum cell removal and the acidic carbohydrate concentration of the algal species, it was observed that the species which had the greatest proportion of acidic carbohydrates per $mm^2$ of polycarbonate membrane had the best cell removal (Table 1B, Figure S2). For instance, MA564, which had the highest proportion of acidic carbohydrates, had the best cell removal among the strains tested, while that of MH and MA555, which had the lowest amount of acidic carbohydrates, had poor cell separation (Figure 3). While only four species were tested to study the impact of acidic carbohydrates, the indications are that the role of these molecules in PosiDAF separation would appear to

warrant further investigation. This was examined in more detail by altering AOM concentration and composition.

(Figure 3)

### 3.4 PosiDAF Jar Tests with altered algal organic matter concentration and composition

#### 3.4.1 Experiment 1:

When the AOM was completely removed from the cell system, it was found that negligible cell separation was achieved for all the strains (Figure 4). On addition of $AOM_C$ back into cell solution, cell separation increased, although to different extents. In jar tests with MA555, CV and MH cells, cell separation reached a maximum value of only 18±4% at a MA555 $AOM_C$ dose of 0.55 $mg \cdot L^{-1}$, 46 ± 3% at a CV $AOM_C$ dose of 0.6 $mg \cdot L^{-1}$ and 28 ± 2% at MH $AOM_C$ dose of 0.4 $mg \cdot L^{-1}$ (Figure 4). In contrast, for MA564 cell system, 95±3% cell separation was observed at a MA564 $AOM_C$ concentration of 0.91 $mg \cdot L^{-1}$ (Figure 4). This was comparable with that observed in PosiDAF tests without extracting the AOM (Yap *et al.* 2014) and confirms that the presence of AOM is critical for separation using PosiDAF, as previously hypothesised by Henderson *et al.* (Henderson *et al.* 2010b).

All the strains demonstrated similar dose response curves with respect to zeta potential. The PosiDAF effluent zeta potential was negative prior to the addition of AOM, with charge reversal occurring at low doses of AOM (Figure 4). The initial negative zeta potential seen in Figure 4, i.e. in the absence of AOM but with 0.0005 $meq \cdot L^{-1}$ of PDADMAC for MA564 and MA555, and 0.004 $meq \cdot L^{-1}$ of PDADMAC for CV and MH, infers that less cationic PDADMAC remains in the DAF effluent in the absence of AOM. Furthermore, as AOM for all the strains has a negative charge (Table 1A), it would be expected that its addition would result in a PosiDAF effluent with greater negative charge; however, the opposite occurred.

(Figure 4)

### 3.4.2 Experiment 2:

When centrifuged, unfiltered MA564 $AOM_C$ was added to the jar tests containing samples of MA555, CV and MH, cell separations greater than 90% were obtained at a doses of 2 $mg \cdot L^{-1}$ and greater (Figure 5 A, B, C). This result shows that AOM extracted from one strain can be used to enhance the cell separation of another.

Dosing of $AOM_{1.50}$ and $AOM_{0.45}$ from MA564 to jar tests containing samples of MA555, CV and MH resulted in lower cell separations in comparison with $AOM_C$. For example, maximum cell separations over 75% for $AOM_{1.50}$ and 60% for $AOM_{0.45}$ were obtained at a dose of 2.0 $mg \cdot L^{-1}$ for the three strains (Figure 5 A, B, C). The 35% reduction in cell removal when using $AOM_{0.45}$ confirms previous observations that high molecular weight biopolymer material was crucial in enhancing the PosiDAF process.

(Figure 5)

### 3.4.3 Experiment 3:

In this experiment, an attempt was made to replicate the results of Experiment 2 by using different sub-cultures of MA555 and $AOM_{1.50}$ generated from MA564, both cultured over a period of one year. On analysis of results, variability was observed in MA555 cell separation for three MA564 $AOM_{1.50}$ replicates (Figure 6). For example, replicates 1, 2 and 3 had maximum cell separations of 96%, 79% and 77%, respectively. This is attributed to the variations in the protein and carbohydrate concentrations in MA564 $AOM_{1.50}$. When comparing their protein concentrations, it was seen that replicate 2 had undetectable levels of protein while replicates 1 and 3 were comparable at 1.9±0.4 and 1.3±0.6 $mg \cdot L^{-1}$, respectively. The carbohydrate concentrations were much higher than the protein concentrations although

they varied significantly; replicate 3 had nearly double the amount of carbohydrates at 16.4±1.2 $mg \cdot L^{-1}$ in comparison to replicate 1. Importantly, the absence of a detectable protein concentration for $AOM_{1.50}$ used in replicate 2 may explain the much higher concentration of AOM required for enhancing the separation. For example, the maximum separation obtained for replicate 2 was comparable to replicate 1 at nearly 5 times the AOM concentration at 2.6 $mg \cdot L^{-1}$ (Figure 6). It is also evident from Figure 6 that the maximum cell separation of 96±3% was obtained for the replicate that had the maximum carbohydrate concentration although its protein concentration was comparable to replicate 1. These results show that variations in the protein and carbohydrate composition in the AOM have a direct impact on PosiDAF performance.

(Figure 6)

## 4 DISCUSSION: The role of AOM in PosiDAF

It is suggested that the AOM and its composition play a significant role in PosiDAF separation effectiveness. In this study, it was observed that cell removals across all strains were poor when PosiDAF was operated in the absence of AOM (Figure 4). However, in the presence of AOM, only MA564 had greater than 95% cell separation (Figure 1). This therefore infers that the AOM in MA555, MH and CV has either a low cell adherence or low polymer binding capability, or both, in comparison to the AOM found in MA564. In the case of MA564, the AOM appeared to provide a physical connection between the polymer-coated bubbles and cells by adhering to or complexing with polymers and attaching to the cell surface. Therefore, understanding the mechanisms behind the AOM's capability to forge a link between the cells and the polymer-coated bubbles is critical to the overall success of PosiDAF.

Comparisons of the AOM from all the species revealed the major differences to be associated with charge and variations in the composition of the AOM size fractions (Table 1A, 1B). Interestingly, while MA564 and MH had comparable charge, cell size and morphology, their cell removals and float characteristics in PosiDAF were found to be vastly different (Figure 1). Therefore, when correlating the cell removal and AOM characterisation results of all the species, it is hypothesised that two factors namely 1) composition of the AOM, and 2) changes to particle (cell) size due to the formation of web-like strands that link several cells, contribute predominantly to the enhanced cell removal in PosiDAF.

The composition of the AOM plays a crucial role in the AOM-cell attachment and formation of large web-like networks that enhance flotation. As both the cells and AOM are negatively charged, the presence of glycoproteins and carbohydrates in the AOM (Henderson *et al.* 2008b) and cell walls (Lee 2008), and their subsequent conjugation due to the presence of multiple binding sites on a glycoprotein surface (Lee *et al.* 1995), are deemed critical for the AOM-cell interactions – a necessity for successful PosiDAF performance, which was seen only in MA564. This would serve as a cogent explanation as to why cell removal increased to greater than 90% despite the addition of negatively charged MA564 AOM to the negatively charged cell suspensions in Experiment 2 jar tests (Figure 5), and why cell removal increased only for MA564 AOM and not the AOM from other strains in Experiment 1 jar tests (Figure 4). In addition, the conjugations between glycoproteins, acidic carbohydrates and carbohydrates are also responsible for the formation of large web-like networks that enhanced flotation of MA564 (Figures 2B to 2E). Such networks have been previously seen in the biomedical field, wherein enhanced binding and bridging interactions were observed (Pfaff *et al.* 2011), especially when studying receptor-ligand recognition and inhibition for cell uptake (Kiessling *et al.* 2000). Therefore, it would be a logical extrapolation to suggest that this

interplay between the aforementioned biomolecules would contribute to the AOM-cell attachments and formation of large web-like structures.

From the development of DAF models such as the white water model performance equation (Haarhoff *et al.* 2004), it is now understood that modifications to the influent conditions such as increasing the particle size can result in elevated particle separations. As a consequence, in PosiDAF, the presence and interaction of the aforementioned suprastructures with polymers is critical for successful flotation. This is supported by the fact that when AOM from MA564 was introduced into the jars containing cells of MA555, MH and CV, the introduced AOM created several networks which increased the apparent size of the particles being separated and consequently increased cell removal to greater than 90% (Figure 5A, B, C). Furthermore, the cell removal did not decrease at doses beyond the optimum level and remained greater than 90% consistently, thereby, supporting the theory that these large polymer-AOM networks enhanced flotation in PosiDAF.

## 5 CONCLUSIONS

The specific conclusions drawn from this work are as follows:

- PosiDAF operated in the absence of AOM resulted in poor cell separation and AOM is therefore considered a necessary system component.
- AOM from MA564 which had the highest MW and acidic carbohydrate content than the other strains improved PosiDAF performance.
- Web-like strands that enhanced flotation of MA564 were analysed. It was seen that conjugation between acidic carbohydrates and proteins was dominant at the strand edge whereas the center of strand had conjugates of proteins with acidic carbohydrates as well as carbohydrates.

- The interplay between proteins, carbohydrates and acidic carbohydrates with the cells and cationic polymers facilitate bubble attachment and flotation.
- A complete investigation of the proteins and carbohydrates present in the AOM from the species tested in this study is recommended to identify the specific proteins and carbohydrates that contribute to enhanced PosiDAF performance.

## ACKNOWLEDGEMENTS

This research was supported via an Australian Research Council's Australia Postgraduate Award (APA), an Australian Department of Education and Training's Research Training Program (RTP) scholarship and the Australian Research Council's Linkage Projects funding scheme (project number LP0990189) which included support from SA Water, Veolia Water, United Water, Melbourne Water and Seqwater. In addition, the authors would like to thank Water Research Australia for the PhD top up scholarship (project number 4025-10) provided to Russell Yap. The authors also acknowledge the support of the UNESCO Centre for Membrane Science and Technology.

## REFERENCES

Anthony, R. J., Ellis, J. T., Sathish, A., Rahman, A., Miller, C. D. and Sims, R. C. (2013). "Effect of coagulant/flocculants on bioproducts from microalgae." Bioresource Technology **149**(0): 65-70.

Bernhardt, H., Hoyer, O., Schell, H. and Lusse, B. (1985). "Reaction Mechanisms Involved in the Influence of Algogenic Organic Matter on Flocculation." Zeitschrift Fur Wasser Und Abwasser Forschung-Journal for Water and Wastewater Research **18**(1): 18-30.

Bernhardt, H., Schell, H., Hoyer, O. and Lüsse, B. (1991). "Influence of algogenic organic substances on flocculation and filtration." WISA **1**(1): 41-57.

Bertocchi, C., Navarini, L., Cesàro, A. and Anastasio, M. (1990). "Polysaccharides from cyanobacteria." Carbohydrate Polymers **12**(2): 127-153.

Bolch, C. S. and Blackburn, S. (1996). "Isolation and purification of Australian isolates of the toxic cyanobacterium Microcystis aeruginosa Kütz." Journal of Applied Phycology **8**(1): 5-13.

Chon, K., Cho, J. and Shon, H. K. (2013). "Advanced characterization of algogenic organic matter, bacterial organic matter, humic acids and fulvic acids." Water Sci Technol **67**(10): 2228-2235.

Coward, T., Lee, J. G. M. and Caldwell, G. S. (2013). "Development of a foam flotation system for harvesting microalgae biomass." Algal Research-Biomass Biofuels and Bioproducts **2**(2): 135-144.

Dubois, M., Gilles, K. A., Hamilton, J. K., Rebers, P. A. and Smith, F. (1956). "Colorimetric method for determination of sugars and related substances." Analytical Chemistry **28**(3): 350-356.

Edzwald, J. K. (2010). "Dissolved air flotation and me." Water Research **44**(7): 2077-2106.

Fang, J., Yang, X., Ma, J., Shang, C. and Zhao, Q. (2010). "Characterization of algal organic matter and formation of DBPs from chlor(am)ination." Water Research **44**(20): 5897-5906.

Frølund, B., Griebe, T. and Nielsen, P. H. (1995). "Enzymatic activity in the activated-sludge floc matrix." Applied Microbiology and Biotechnology **43**(4): 755-761.

Giordano, M., Kansiz, M., Heraud, P., Beardall, J., Wood, B. and McNaughton, D. (2001). "Fourier Transform Infrared spectroscopy as a novel tool to investigate changes in intracellular macromolecular pools in the marine microalga Chaetoceros muellerii (Bacillariophyceae)." Journal of Phycology **37**(2): 271-279.

Gonzalez-Torres, A., Rich, A. M., Marjo, C. E. and Henderson, R. K. (2017). "Evaluation of biochemical algal floc properties using Reflectance Fourier-Transform Infrared Imaging." Algal Research **27**(Supplement C): 345-355.

Haarhoff, J. and Edzwald, J. K. (2004). "Dissolved air flotation modelling: Insights and shortcomings." Journal of Water Supply: Research and Technology - AQUA **53**(3): 127-150.

Hadjoudja, S., Deluchat, V. and Baudu, M. (2010). "Cell surface characterisation of Microcystis aeruginosa and Chlorella vulgaris." Journal of Colloid and Interface Science **342**(2): 293-299.

Han, M., Kim, M. and Ahn, H. (2006). "Effects of surface charge, micro-bubble size and particle size on removal efficiency of electro-flotation." Water science and technology **53**(7): 127-132.

Henderson, R., Parsons, S. A. and Jefferson, B. (2008a). "The impact of algal properties and pre-oxidation on solid–liquid separation of algae." Water Research **42**(8–9): 1827-1845.

Henderson, R. K., Baker, A., Parsons, S. A. and Jefferson, B. (2008b). "Characterisation of algogenic organic matter extracted from cyanobacteria, green algae and diatoms." Water Research **42**(13): 3435-3445.

Henderson, R. K., Parsons, S. A. and Jefferson, B. (2008c). "Surfactants as bubble surface modifiers in the flotation of algae: Dissolved air flotation that utilizes a chemically modified bubble surface." Environmental Science and Technology **42**(13): 4883-4888.

Henderson, R. K., Parsons, S. A. and Jefferson, B. (2009). "The potential for using bubble modification chemicals in dissolved air flotation for algae removal." Separation Science and Technology **44**(9): 1923-1940.

Henderson, R. K., Parsons, S. A. and Jefferson, B. (2010a). "The impact of differing cell and algogenic organic matter (AOM) characteristics on the coagulation and flotation of algae." Water Research **44**(12): 3617-3624.

Henderson, R. K., Parsons, S. A. and Jefferson, B. (2010b). "Polymers as bubble surface modifiers in the flotation of algae." Environmental Technology **31**(7): 781-790.

Huber, S. A., Balz, A., Abert, M. and Pronk, W. (2011). "Characterisation of aquatic humic and non-humic matter with size-exclusion chromatography - organic carbon detection - organic nitrogen detection (LC-OCD-OND)." Water Research **45**(2): 879-885.

Kehr, J.-C. and Dittmann, E. (2015). "Biosynthesis and function of extracellular glycans in cyanobacteria." Life **5**(1): 164-180.

Kempeneers, S., Van Menxel, F. and Gille, L. (2001). "A decade of large scale experience in dissolved air flotation." Water science and technology **43**(8): 27-34.

Kiessling, L. L., Gestwicki, J. E. and Strong, L. E. (2000). "Synthetic multivalent ligands in the exploration of cell-surface interactions." Current Opinion in Chemical Biology **4**(6): 696-703.

Lee, N., Amy, G. and Croué, J.-P. (2006). "Low-pressure membrane (MF/UF) fouling associated with allochthonous versus autochthonous natural organic matter." Water Research **40**(12): 2357-2368.

Lee, R. E. (2008). "Phycology." (fourth ed.), Cambridge University Press, Cambridge, UK, p. 547.

Lee, Y. C. and Lee, R. T. (1995). "Carbohydrate-Protein Interactions: Basis of Glycobiology." Accounts of Chemical Research **28**(8): 321-327.

Lin, J. T. (2007). "HPLC separation of acyl lipid classes." Journal of Liquid Chromatography and Related Technologies **30**(14): 2005-2020.

Malley, J. P. (1995). "The use of selective and direct DAF for removal of particulate contaminants in drinking water treatment." Water Science and Technology **31**(3–4): 49-57.

Mecozzi, M., Acquistucci, R., Di Noto, V., Pietrantonio, E., Amici, M. and Cardarilli, D. (2001). "Characterization of mucilage aggregates in Adriatic and Tyrrhenian Sea: structure

similarities between mucilage samples and the insoluble fractions of marine humic substance." Chemosphere **44**(4): 709-720.

Mopper, K., zhou, J., Sri Ramana, K., passow, U., dam, H. G. and Drapeau, D. T. (1995). "The role of surface-active carbohydrates in the flocculation of a diatom bloom in a mesocosm." Deep Sea Research Part II: Topical Studies in Oceanography **42**(1): 47-73.

Murdock, J. N. and Wetzel, D. L. (2009). "FT-IR microspectroscopy enhances biological and ecological analysis of algae." Applied Spectroscopy Reviews **44**(4): 335-361.

Oliveira, C. and Rubio, J. (2012). "Kaolin aerated flocs formation assisted by polymer-coated microbubbles." International Journal of Mineral Processing **106-109**: 31-36.

Passow, U. (2002). "Transparent exopolymer particles (TEP) in aquatic environments." Progress in Oceanography **55**(3–4): 287-333.

Passow, U. and Alldredge, A. L. (1995). "A dye-binding assay for the spectrophotometric measurement of transparent exopolymer particles (TEP)." Limnology and Oceanography **40**(7): 1326-1335.

Pfaff, A., Barner, L., Müller, A. H. E. and Granville, A. M. (2011). "Surface modification of polymeric microspheres using glycopolymers for biorecognition." European Polymer Journal **47**(4): 805-815.

Pieterse, A. and Cloot, A. (1997). "Algal cells and coagulation, flocculation and sedimentation processes." Water Science and Technology **36**(4): 111-118.

Pivokonsky, M., Kloucek, O. and Pivokonska, L. (2006). "Evaluation of the production, composition and aluminum and iron complexation of algogenic organic matter." Water Research **40**(16): 3045-3052.

Pivokonsky, M., Naceradska, J., Kopecka, I., Baresova, M., Jefferson, B., Li, X. and Henderson, R. (2016). "The impact of algogenic organic matter on water treatment plant

operation and water quality: A review." Critical Reviews in Environmental Science and Technology **46**(4): 291-335.

Pivokonsky, M., Safarikova, J., Baresova, M., Pivokonska, L. and Kopecka, I. (2014). "A comparison of the character of algal extracellular versus cellular organic matter produced by cyanobacterium, diatom and green alga." Water Research **51**: 37-46.

Qu, F., Liang, H., He, J., Ma, J., Wang, Z., Yu, H. and Li, G. (2012). "Characterization of dissolved extracellular organic matter (dEOM) and bound extracellular organic matter (bEOM) of Microcystis aeruginosa and their impacts on UF membrane fouling." Water Research **46**(9): 2881-2890.

Shi, Y., Yang, J., Ma, J. and Luo, C. (2017). "Feasibility of bubble surface modification for natural organic matter removal from river water using dissolved air flotation." Frontiers of Environmental Science & Engineering **11**(6): 10.

Sigee, D. C., Dean, A., Levado, E. and Tobin, M. J. (2002). "Fourier-transform infrared spectroscopy of Pediastrum duplex: characterization of a micro-population isolated from a eutrophic lake." European Journal of Phycology **37**(1): 19-26.

Sudharsan, S., Subhapradha, N., Seedevi, P., Shanmugam, V., Madeswaran, P., Shanmugam, A. and Srinivasan, A. (2015). "Antioxidant and anticoagulant activity of sulfated polysaccharide from Gracilaria debilis (Forsskal)." International Journal of Biological Macromolecules **81**: 1031-1038.

Takaara, T., Sano, D., Konno, H. and Omura, T. (2007). "Cellular proteins of Microcystis aeruginosa inhibiting coagulation with polyaluminum chloride." Water Research **41**(8): 1653-1658.

Villacorte, L. O., Ekowati, Y., Calix-Ponce, H. N., Schippers, J. C., Amy, G. L. and Kennedy, M. D. (2015a). "Improved method for measuring transparent exopolymer particles (TEP) and their precursors in fresh and saline water." Water Research **70**: 300-312.

Villacorte, L. O., Ekowati, Y., Neu, T. R., Kleijn, J. M., Winters, H., Amy, G., Schippers, J. C. and Kennedy, M. D. (2015b). "Characterisation of algal organic matter produced by bloom-forming marine and freshwater algae." Water Research **73**: 216-230.

Weschler, M. K., Barr, W. J., Harper, W. F. and Landis, A. E. (2013). "Process Energy Comparison for the Production and Harvesting of Algal Biomass as a Biofuel Feedstock." Bioresource Technology **153C**: 108-115.

Yap, R. K. L., Whittaker, M., Diao, M., Stuetz, R. M., Jefferson, B., Bulmuş, V., Peirson, W. L., Nguyen, A. and Henderson, R. K. (2014). "Hydrophobically-associating cationic polymers as micro-bubble surface modifiers in dissolved air flotation for cyanobacteria cell separation." Water Research **61C**: 253-262.

Zhang, X., Bishop, P. L. and Kinkle, B. K. (1999). "Comparison of extraction methods for quantifying extracellular polymers in biofilms." Water science and technology **39**(7): 211-218.

Zhang, X., Fan, L. and Roddick, F. A. (2013). "Understanding the fouling of a ceramic microfiltration membrane caused by algal organic matter released from Microcystis aeruginosa." Journal of Membrane Science **447**: 362-368.

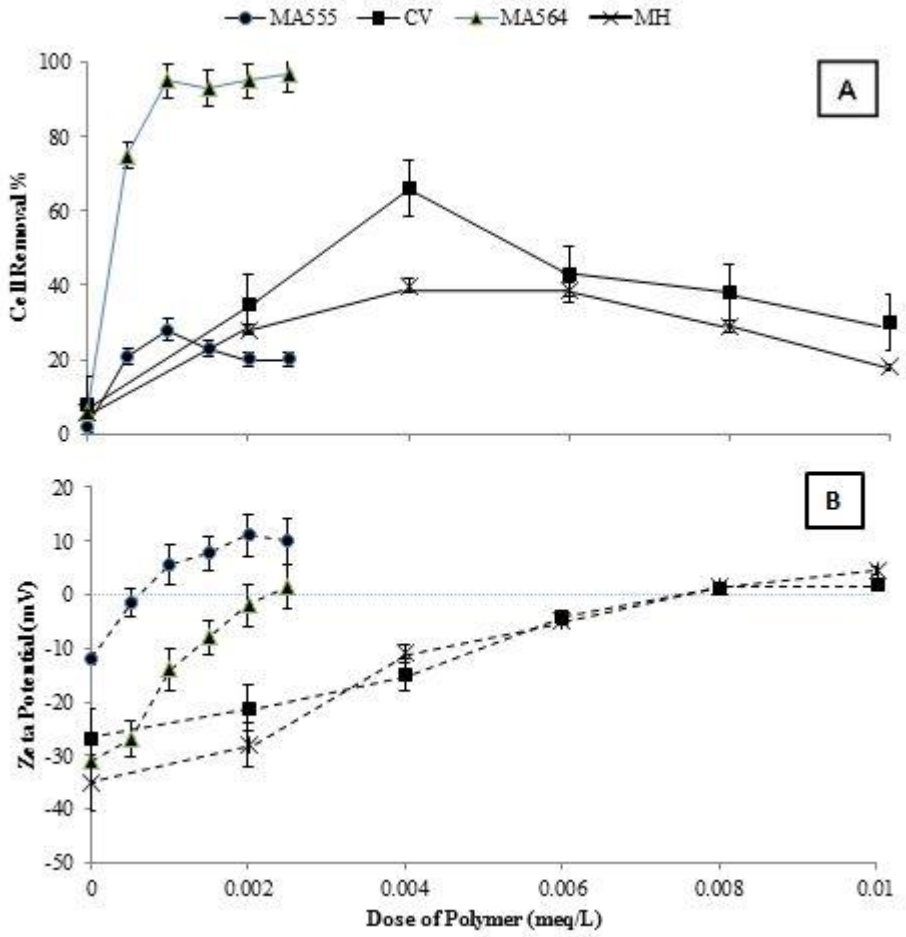


Figure 1. Comparison of PosiDAF performance with PDADMAC on CV, MH, MA555 and MA564; A – Cell removal efficiency and B – Zeta Potential of effluent Vs Dose of PDADMAC;

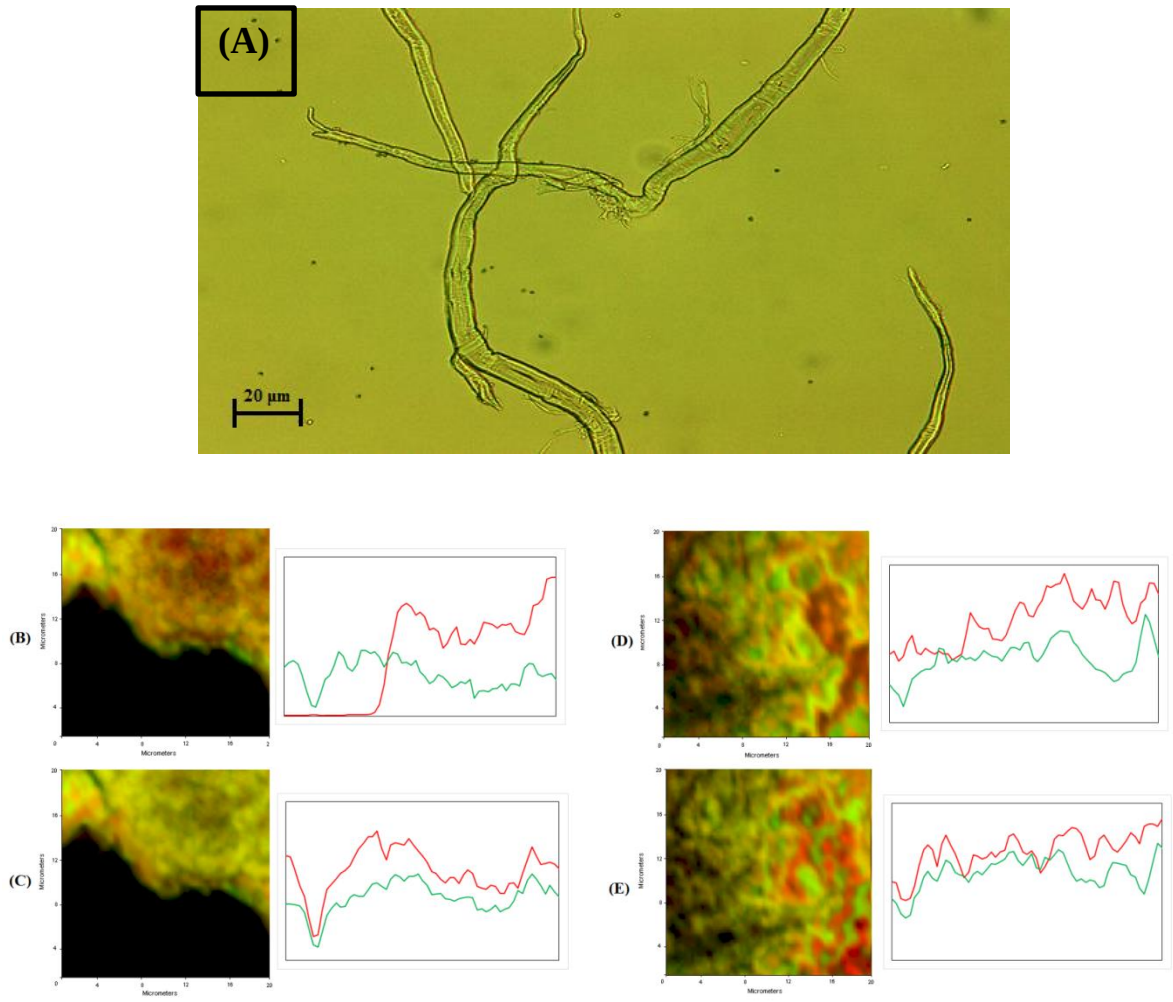


Figure 2. Image (A) - Strands from MA564 viewed under a microscope. Images (B), (C) - 20 x 20 $\mu m^2$ FTIR images of strand edge with the corresponding cross section spectra of the strand edge. Images (D), (E) - 20 x 20 $\mu m^2$ FTIR images of strand center with the corresponding cross section spectra of the center of the strand. Red regions in images (B) to (E) are the relative intensities of the protein amide I peak at 1630 $cm^{-1}$. Green regions in (B) and (D) are the relative intensities of the carbohydrate C-O vibration at 1030 $cm^{-1}$, and in (C) and (E), are the relative intensities of the acidic carbohydrate anion $COO^-$ vibration at 1330 $cm^{-1}$. The regions of orange and yellow in (B) to (E) are the overlaps of the respective chemical regions in the image. For full dataset, please see supporting information Figure S3.4.

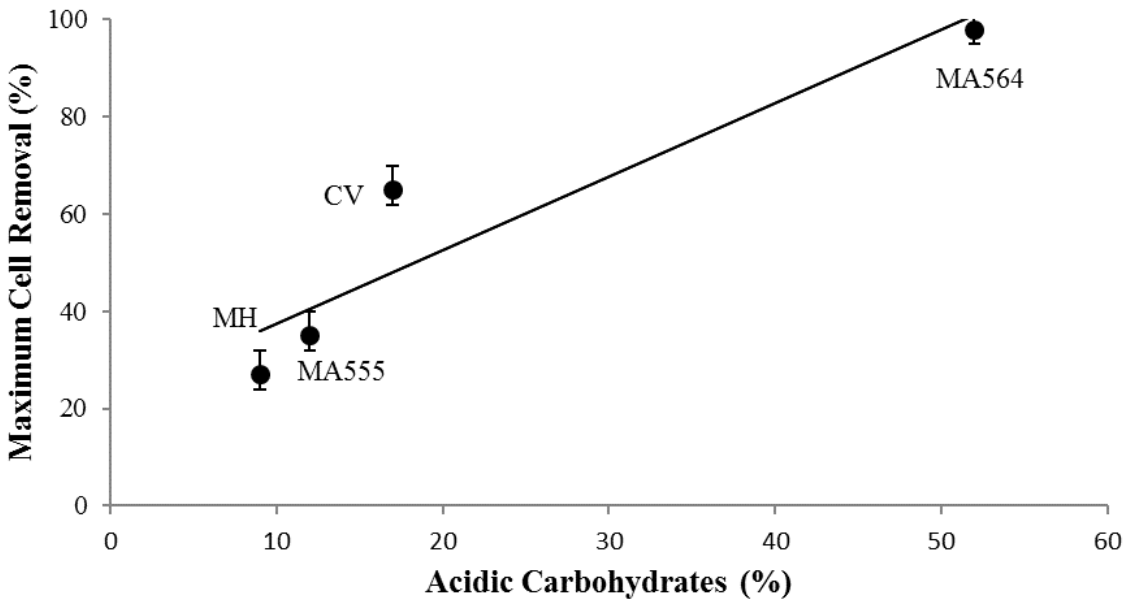


Figure 3. Comparison of maximum cell removal of CV, MH, MA555 and MA564 vs the acidic carbohydrates detected by Alcian Blue staining. Acidic carbohydrate concentration represented as percent area per 0.18 $mm^2$ of polycarbonate membrane.

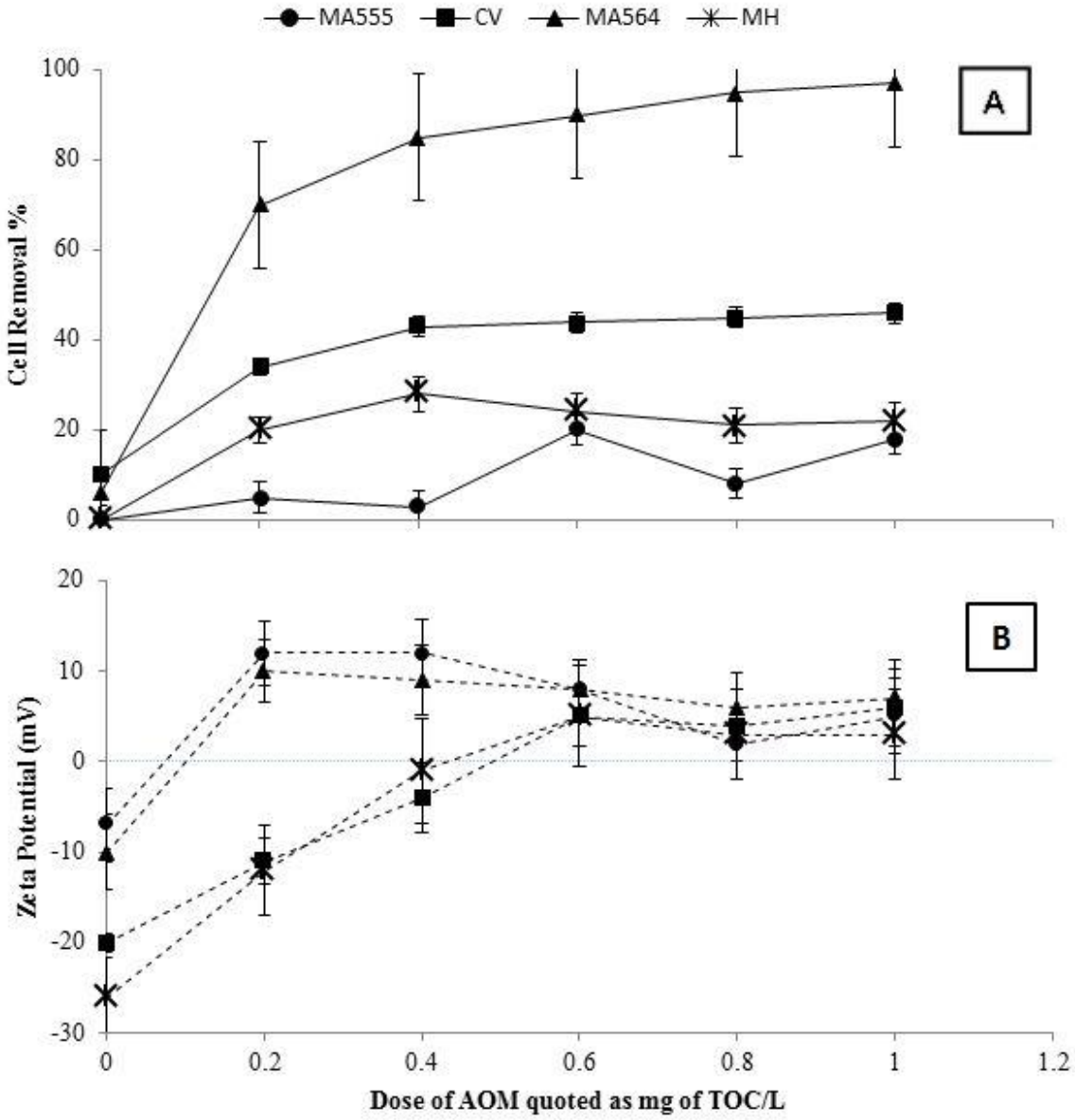


Figure 4. PosiDAF jar test outcomes with PDADMAC for CV, MH, MA555 and MA564 cells with their respective AOM added to jars at various concentrations; A – Cell removal efficiency and B – Zeta Potential of effluent Vs Dose of AOM; Concentrations of PDADMAC for MA555, MA564 were 0.0005 meq/L and for CV, MH were 0.004 meq/L.

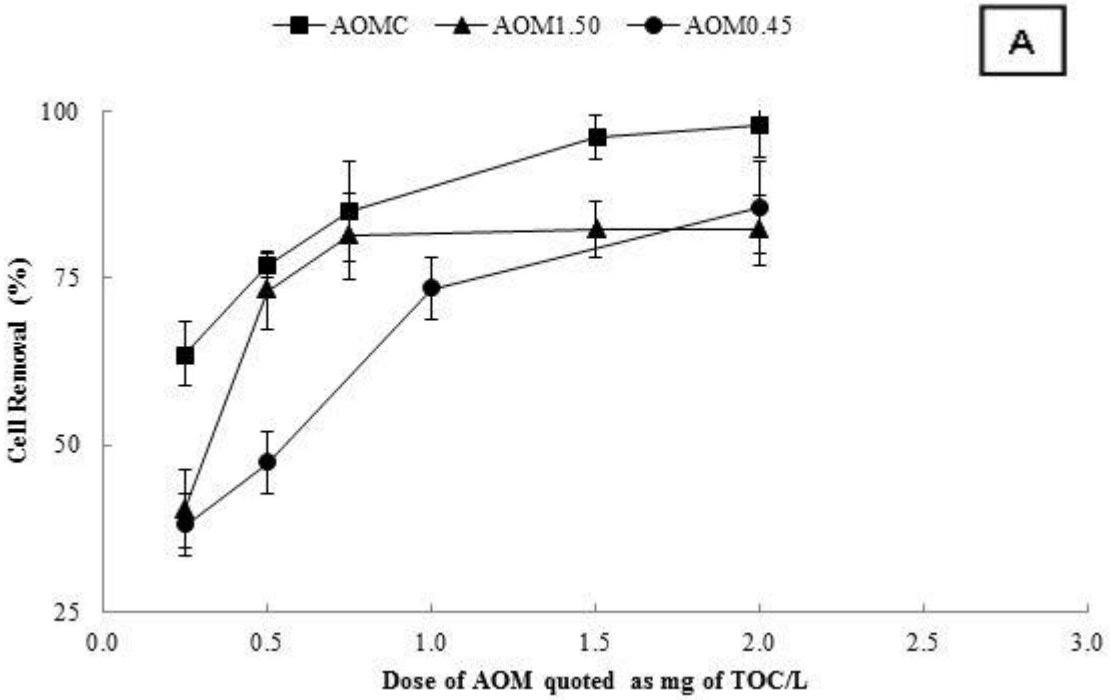
AOMC
AOM1.50
AOM0.45
A
100
75
50
25
Cell Removal (%)
0.0
0.5
1.0
1.5
2.0
2.5
3.0
Dose of AOM quoted as mg of TOC/L

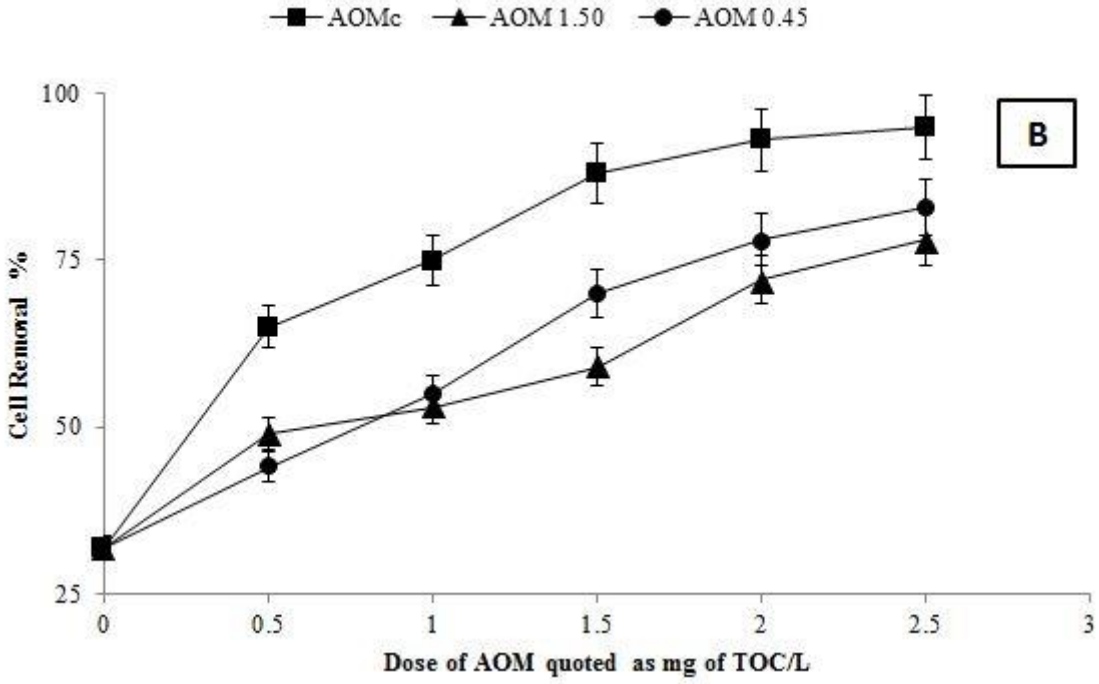
AOMc
AOM 1.50
AOM 0.45
B
100
75
50
25
Cell Removal %
0
0.5
1
1.5
2
2.5
3
Dose of AOM quoted as mg of TOC/L

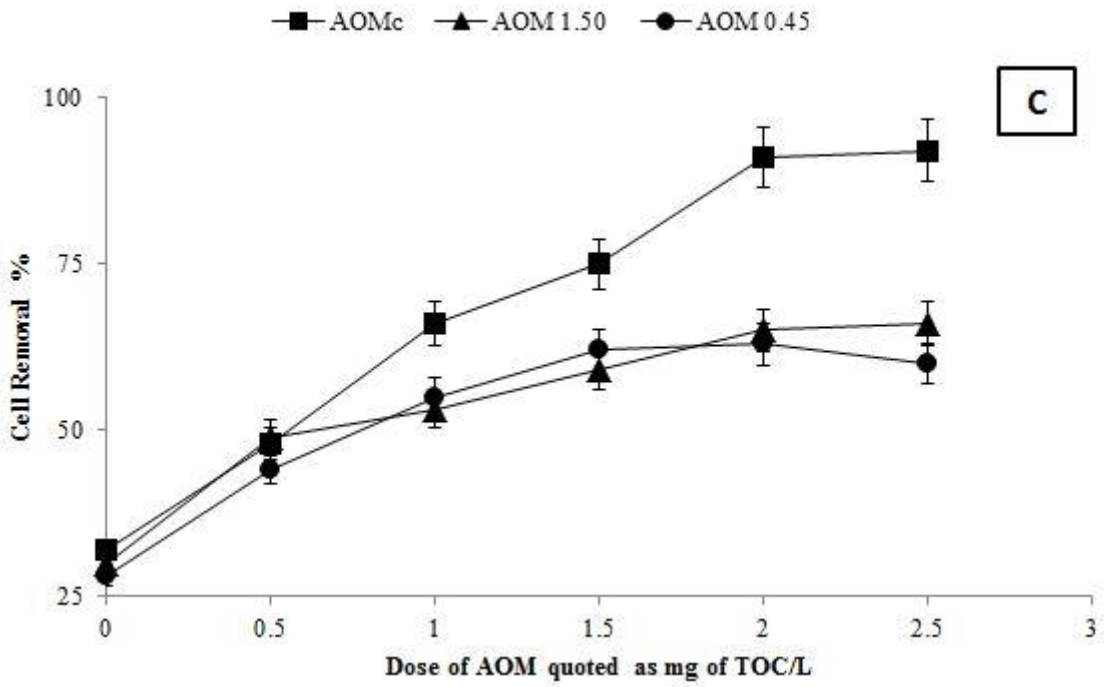


Figure 5. Cell separation as a function of AOM dose for Experiment 2 jar tests of A – MA555; B - CV; C – MH, using MA564 AOM to enhance flotation.

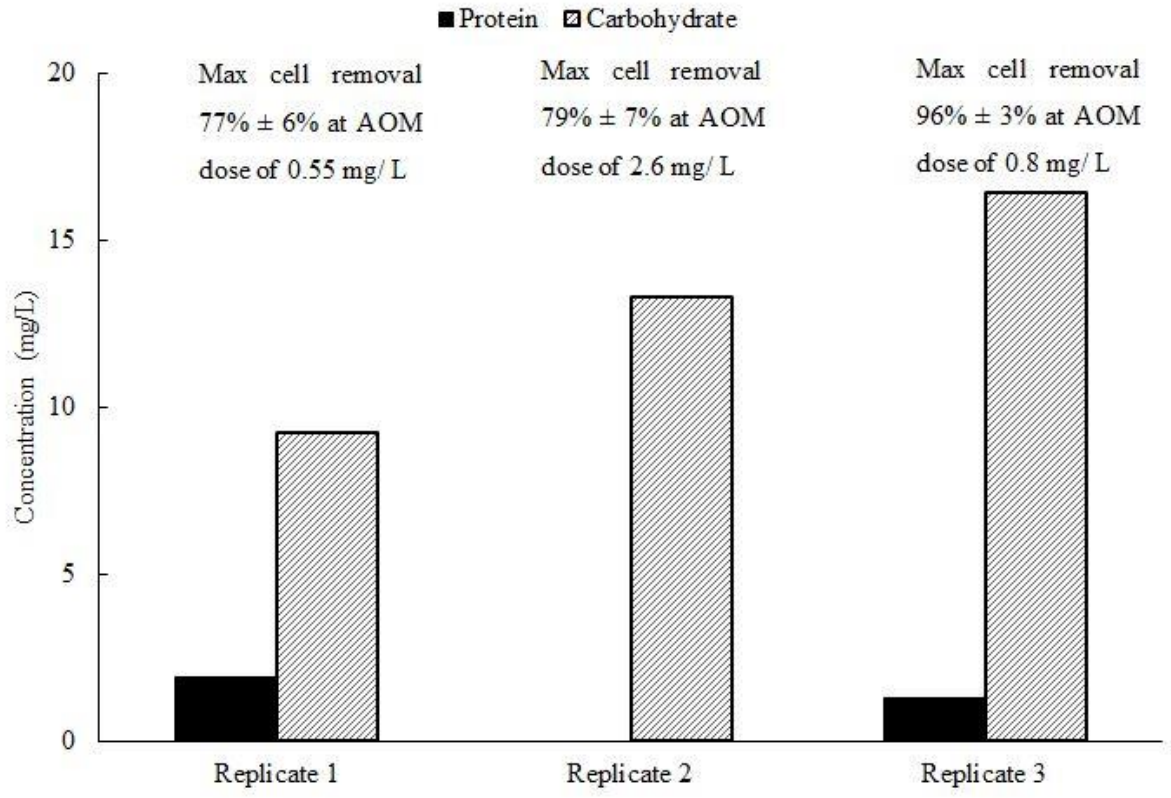


Figure 6. Protein and carbohydrate concentrations of MA564 $AOM_{1.50}$ while using it as a flotation enhancer for MA555 in PosiDAF. Stock MA564 and MA555 used in these experiments were recultured from three different parent cultures over an extended period of time (approx. 1 year).

Supporting information

Table S1. A comparison of the biopolymers, humic substance, building blocks and LMW neutrals as determined from LC-OCD analysis of $AOM_{0.45}$

| Strain | Biopolymers | Humic Substances | Building Blocks | LMW Neutrals |
|---|---|---|---|---|
| MA555 | 12.7% | 13.0% | 22.9% | 31.2% |
| MA564 | 18.5% | 14.7% | 44.6% | 21.3% |
| CV | 19.3% | 10.2% | 19.1% | 23.7% |
| MH | 5.4% | 11.4% | 38.5% | 44.7% |

Table S2. Band assignment- FTIR, adapted from (Giordano *et al.* 2001, Mecozzi *et al.* 2001, Sigee *et al.* 2002, Lee *et al.* 2006, Murdock *et al.* 2009, Chon *et al.* 2013, Sudharsan *et al.* 2015).

| **Peak** | **Wavenumber range[1] ($cm^{-1}$)** | **Functional group** | **Biomolecular origin** |
|---|---|---|---|
| 1 | 3500-3100 | Hydrogen-bonded OH stretch | Polysaccharides |
| 2 | 2950-2850 | Aliphatic C-H stretch | Lipid |
| 3 | 1750-1700 | Ester, ketone and carboxylic acid C=O stretch | Lipid, chlorophyll, carotenoid pigments |
| 4 | 1660-1610 | Amide C=O stretch | Protein (Amide I) |
| | | $_{V}(COO)_{asym}$ | |
| 5 | 1580-1550 | Amide C-N stretch and N-H bend | Protein (Amide II), Polysaccharides |
| 6 | 1370-1310 | Carboxylate anion stretch $COO^-$ | Polysaccharides (charged) |
| | | Amide CN and NH vibrations | Protein (Amide III) |
| | | $CH_2$ deformation | Lipid |
| 7 | 1260-1230 | Sulphated ester stretch R-O-$SO_3^-$ | Polysaccharides (charged) |
| 8 | 1150-1130 | Ether C-O-C stretch | Polysaccharides |
| 9 | 1100-1050 | Alcohol C-O stretch | Polysaccharides |
| | | Phosphate ester P=O stretch | Nucleic acids |

[1] The position of these assignments can vary in the literature. Individual bands may have attributions from a number of molecular groups.

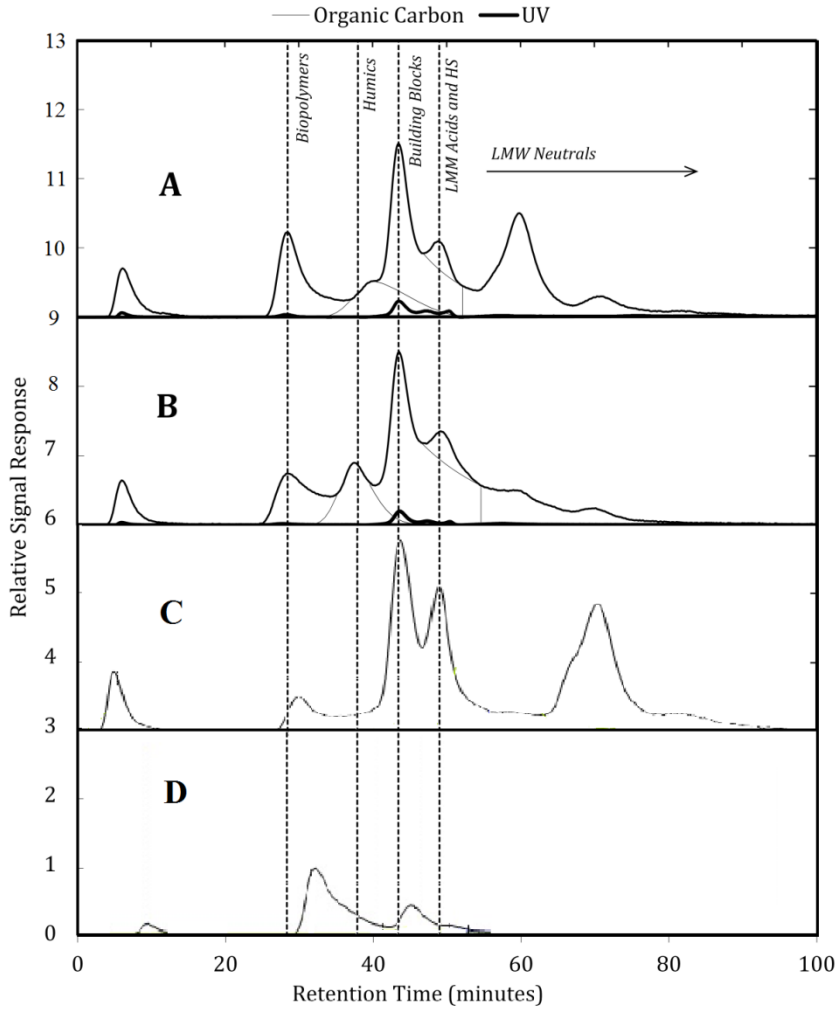


Figure S1. LC-OCD and UV results for (A) MA555 (B) MA564 (C) MH (D) CV.

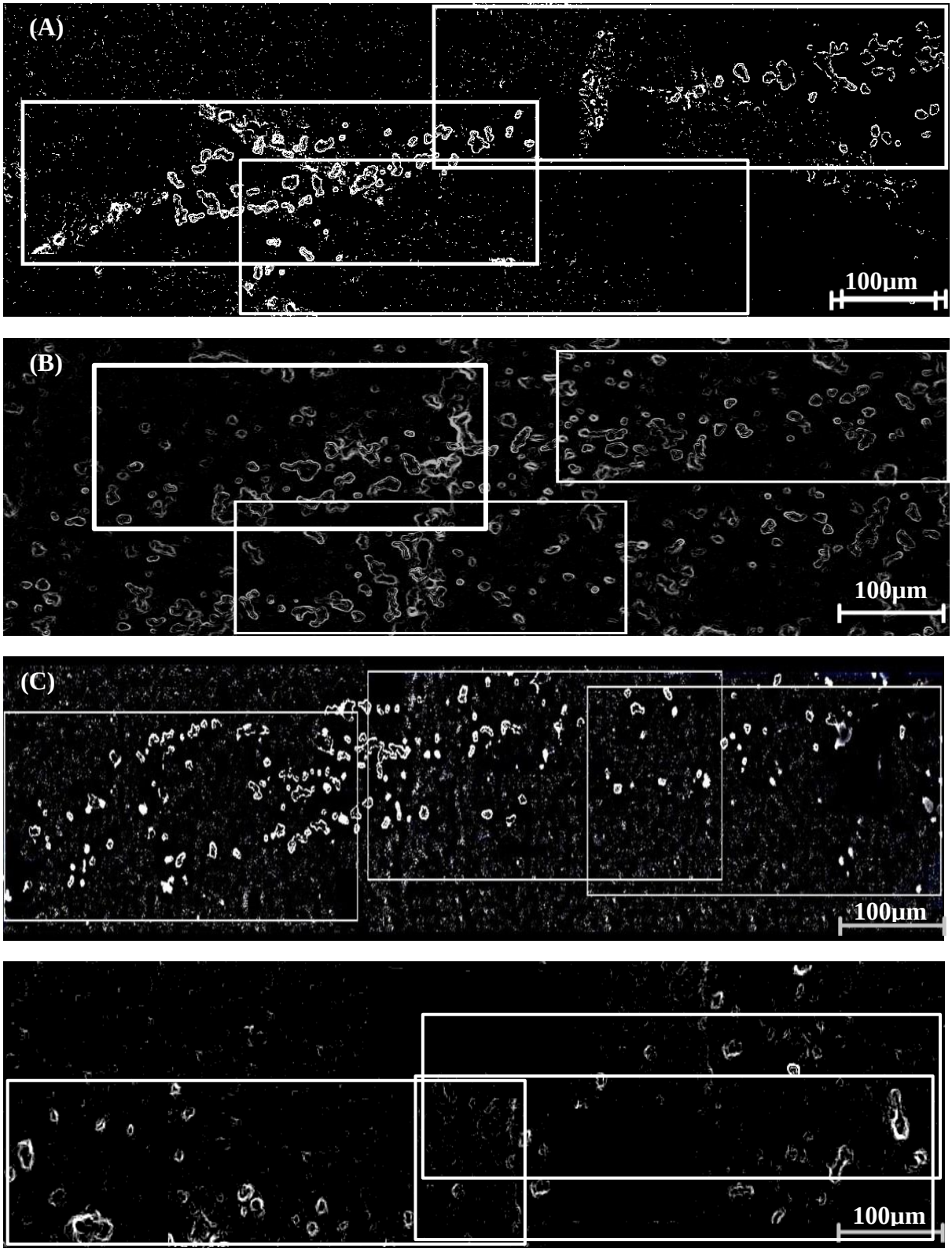


Figure S2 – TEP stained with Alcian blue for (A) – MA555, (B) – MA564/01, (C) – CV, (D) – MH.

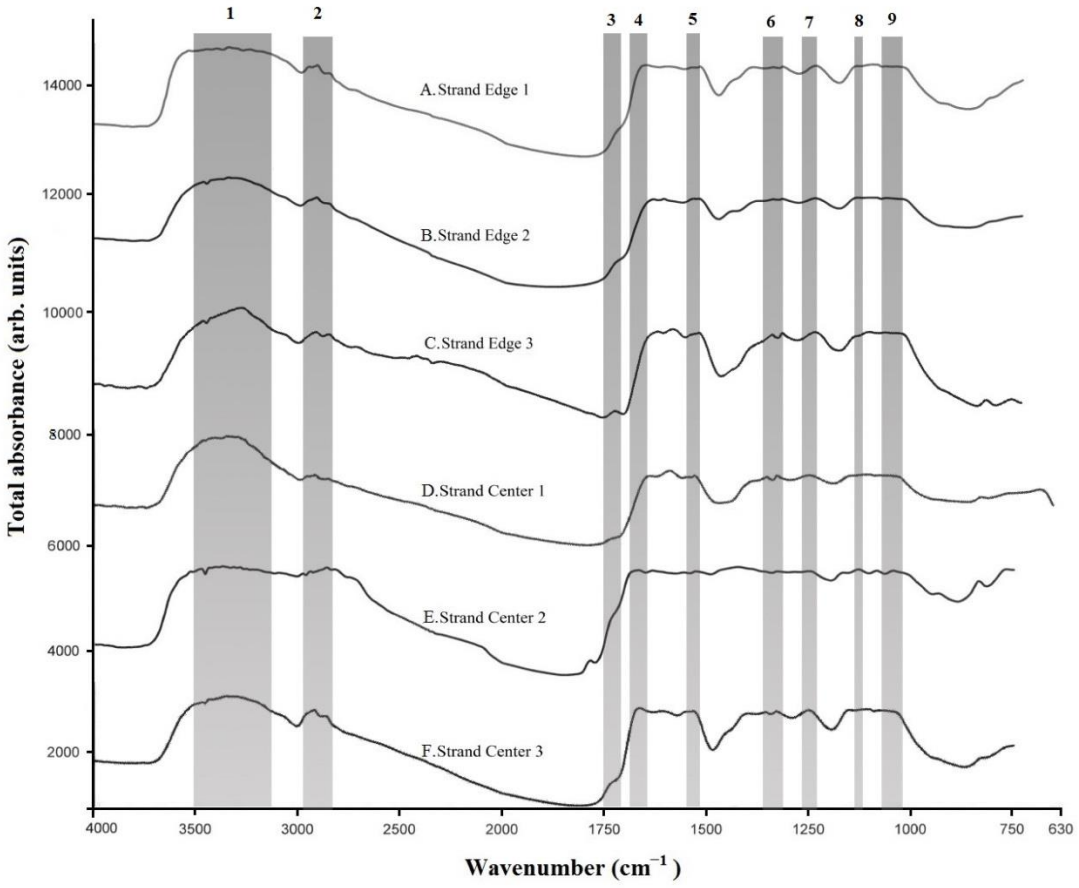


Figure S3. Infrared absorbance spectra as a total of all 4096 individual spectra in each image, with assignment of major peaks numbered according to Table S1. Spectra are presented as absorbance vs wavenumber ($cm^{-1}$), and have been baseline corrected and arbitrarily scaled for comparison.

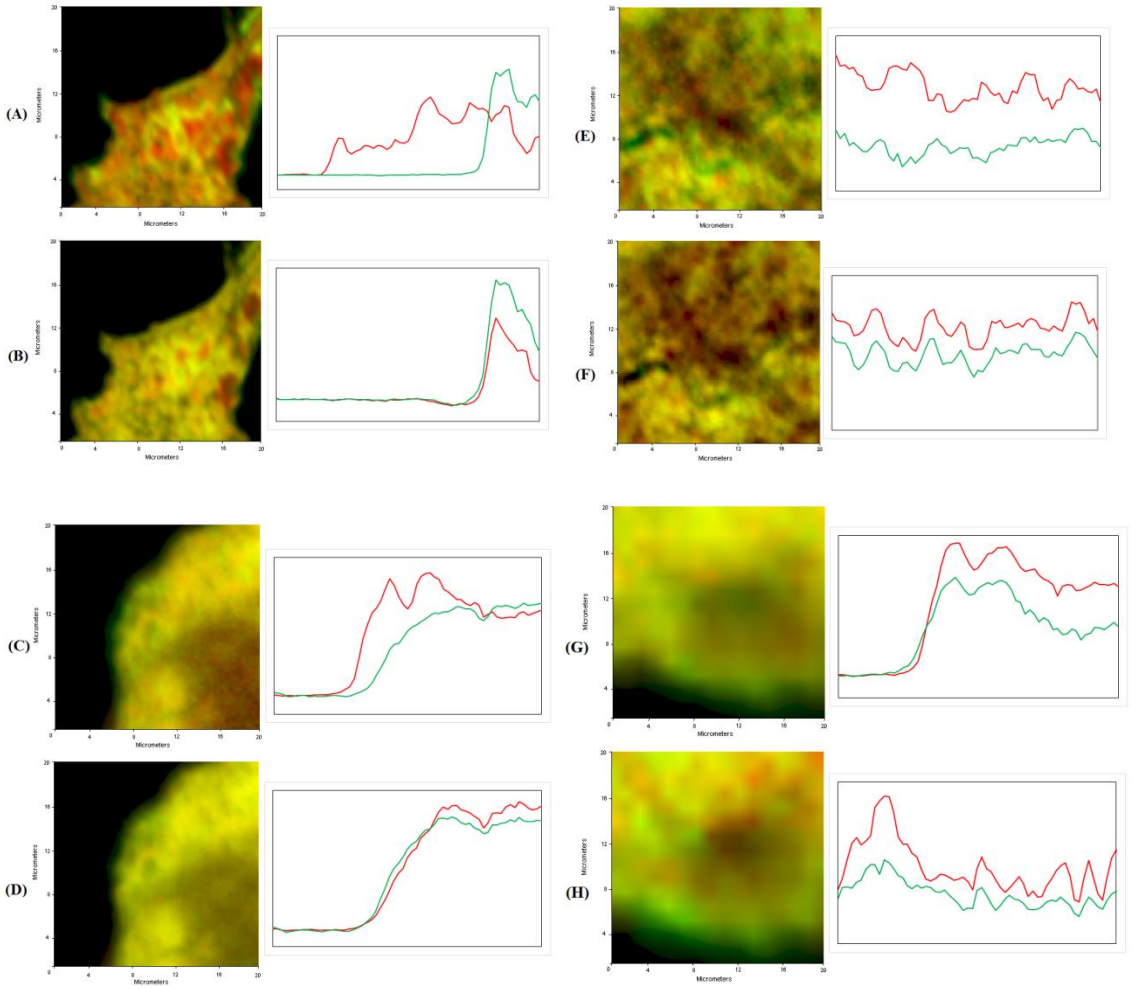


Figure S4. Images (A) to (D) - 20 x 20 $\mu m^2$ FTIR images of strand edge with the corresponding cross section spectra of the strand edge. Images (E) to (H) - 20 x 20 $\mu m^2$ FTIR images of strand center with the corresponding cross section spectra of the center of the strand. Red regions in images (A) to (H) are the relative intensities of the protein amide I peak at 1630 $cm^{-1}$. Green regions in (A), (C), (E), (G) are the relative intensities of the carbohydrate C-O vibration at 1030 $cm^{-1}$, and in (B), (D), (F), (H) are the relative intensities of the acidic carbohydrate anion $COO^-$ vibration at 1330 $cm^{-1}$. The regions of orange and yellow in (A) to (H) are the overlaps of the respective chemical regions in the image.

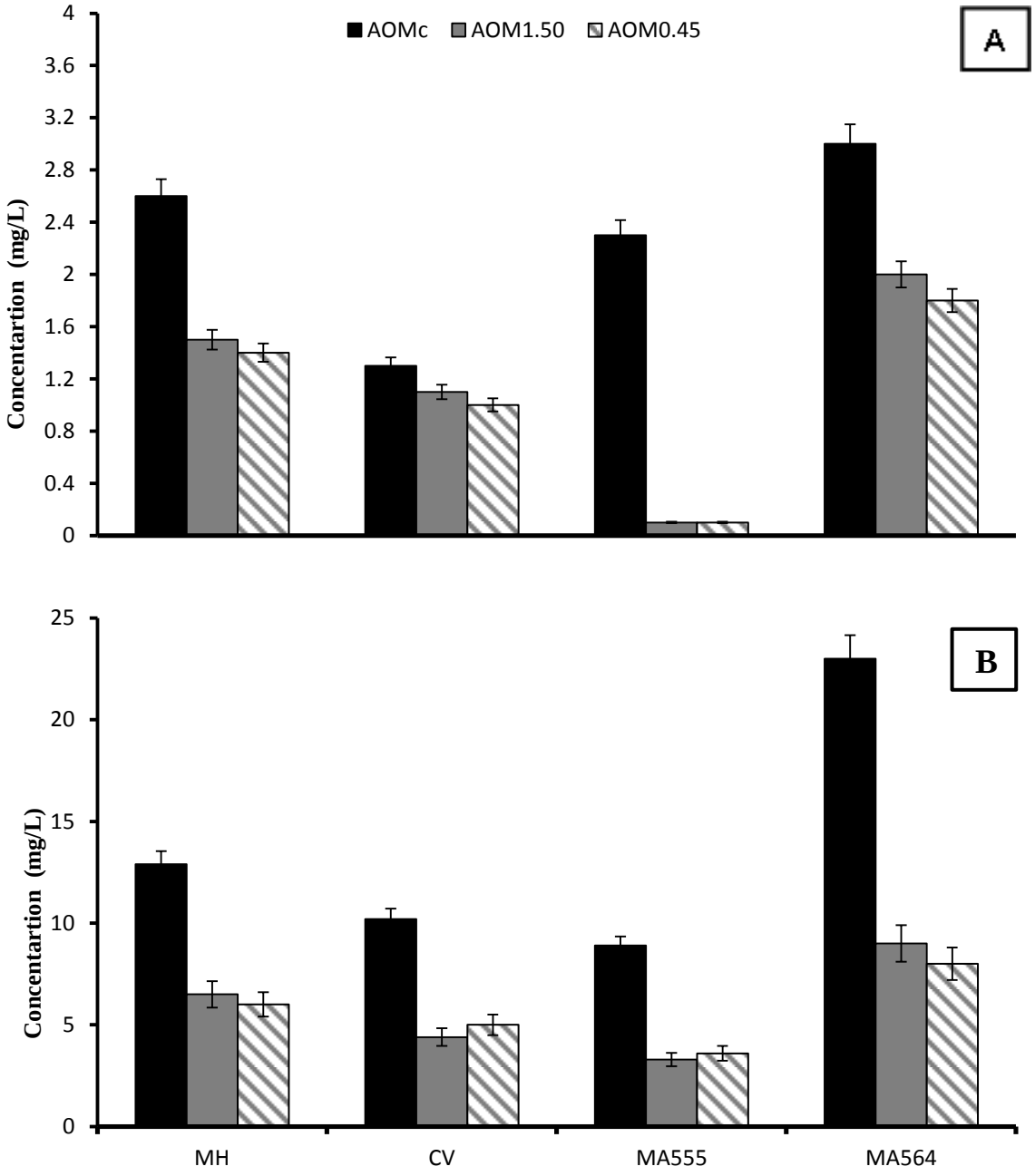


Figure S5. (A) Protein; (B) carbohydrate concentrations of the respective filtered fractions of AOM from MH, CV, MA555 and MA564.

**References**

Chon, K., J. Cho and H. K. Shon (2013). "Advanced characterization of algogenic organic matter, bacterial organic matter, humic acids and fulvic acids." Water Sci Technol **67**(10): 2228-2235.

Giordano, M., M. Kansiz, P. Heraud, J. Beardall, B. Wood and D. McNaughton (2001). "Fourier Transform Infrared spectroscopy as a novel tool to investigate changes in intracellular macromolecular pools in the marine microalga Chaetoceros muellerii (Bacillariophyceae)." Journal of Phycology **37**(2): 271-279.

Lee, N., G. Amy and J.-P. Croué (2006). "Low-pressure membrane (MF/UF) fouling associated with allochthonous versus autochthonous natural organic matter." Water Research **40**(12): 2357-2368.

Mecozzi, M., R. Acquistucci, V. Di Noto, E. Pietrantonio, M. Amici and D. Cardarilli (2001). "Characterization of mucilage aggregates in Adriatic and Tyrrhenian Sea: structure similarities between mucilage samples and the insoluble fractions of marine humic substance." Chemosphere **44**(4): 709-720.

Murdock, J. N. and D. L. Wetzel (2009). "FT-IR Microspectroscopy Enhances Biological and Ecological Analysis of Algae." Applied Spectroscopy Reviews **44**(4): 335-361.

Sigee, D. C., A. Dean, E. Levado and M. J. Tobin (2002). "Fourier-transform infrared spectroscopy of Pediastrum duplex: characterization of a micro-population isolated from a eutrophic lake." European Journal of Phycology **37**(1): 19-26.

Sudharsan, S., N. Subhapradha, P. Seedevi, V. Shanmugam, P. Madeswaran, A. Shanmugam and A. Srinivasan (2015). "Antioxidant and anticoagulant activity of sulfated polysaccharide from Gracilaria debilis (Forsskal)." International Journal of Biological Macromolecules **81**: 1031-1038.

Table 1A. Physical and charge characteristics of the cultures and different AOM fractions extracted from MA555, MA564, MH and CV in comparison with previously tested UK strains of MA (CCAP 1450/3) and CV (CCAP 211/11B). All assays were done in triplicate.

| **Properties** | **Diameter** ^ | **Average cell concentration at the onset of stationary phase** | **Zeta Potential** | | | | **Charge Density** | | | |
|---|---|---|---|---|---|---|---|---|---|---|
| | | | Culture | ($AOM_C$) | ($AOM_{1.50}$) | ($AOM_{0.45}$) | Culture | ($AOM_C$) | ($AOM_{1.50}$) | ($AOM_{0.45}$) |
| **Units** | μm | $\times 10^7$ cells $mL^{-1}$ | mV | mV | mV | mV | $\times 10^{-7}$ meq $cell^{-1}$ | $\times 10^{-7}$ meq $cell^{-1}$ | $\times 10^{-7}$ meq $cell^{-1}$ | $\times 10^{-7}$ meq $cell^{-1}$ |
| **MA555** | 3.0 ± 0.7 | 1.79 ± 0.08 | -17.0 ± 1.0 | -8.0 ± 1.6 | -9.0 ± 3.6 | -8.3 ± 1.9 | -9.3 ± 0.6 | -5.6 ± 1.3 | -4.8 ± 0.2 | -4.3 ± 1.0 |
| **MA564** | 3.1 ± 0.6 | 2.01 ± 0.12 | -32.8 ± 0.6 | -26.2 ± 5.1 | -22.7 ± 6.6 | -20.2 ± 1.8 | -14.1 ± 0.8 | -7.9 ± 1.8 | -6.1 ± 0.5 | -5.8 ± 3.0 |
| **CV** | 5.2 ± 0.6 | 1.3 ± 0.3 | -24.6 † 4.3 | -21.3 ± 4.3 | -17.1 ± 2.4 | -15.7 ± 1.8 | - 2.8 ± 0.6 | -1.9 ± 0.22 | -1.75 ± 1.5 | -1.2 ± 0.02 |
| **MH** | 2.8 ± 0.5 | 0.9 ± 0.2 | -35.1 ± 5.6 | -28.9 ± 2.9 | -25.8 ± 2.3 | -21 ± 3.4 | -14.8 ± 0.6 | - 8.4 ± 0.8 | - 7.6 ± 0.3 | - 6.96 ± 0.87 |
| **MA (UK)** †‡ | 5.4 ± 0.8 † | - | -19.8 ± 1.5 † | - | - | -21.5 ǂ | -0.02 ǂ | - | - | -0.01 ǂ |
| **CV (UK)** †‡ | 4 ± 1.1 † | - | -32.3 ± 0.6 † | - | - | -18.9 ǂ | -0.85 ǂ | - | - | -0.72 ǂ |

'-' indicates no data available

† Data obtained or calculated from Henderson *et al.*[22]

‡ Data obtained or calculated from Henderson *et al.*[30]

Table 1B. Chemical composition of the different AOM fractions extracted from MA555, MA564, MH and CV in comparison with previously tested UK strains of MA (CCAP 1450/3) and CV (CCAP-211/11B). All assays were done in triplicate.

| **Properties** | **TOC/DOC** | | | **Carbohydrate : Organic carbon[a]** | | | **Protein : Organic carbon[a]** | | | **Acidic carbohydrate concentration** |
|---|---|---|---|---|---|---|---|---|---|---|
| | ($AOM_C$) | ($AOM_{1.50}$) | ($AOM_{0.45}$) | ($AOM_C$) | ($AOM_{1.50}$) | ($AOM_{0.45}$) | ($AOM_C$) | ($AOM_{1.50}$) | ($AOM_{0.45}$) | |
| **Units** | $x10^{-10}$ mg $cell^{-1}$ | $x10^{-10}$ mg $cell^{-1}$ | $x10^{-10}$ mg $cell^{-1}$ | mg $mg^{-1}$ | mg $mg^{-1}$ | mg $mg^{-1}$ | mg $mg^{-1}$ | mg $mg^{-1}$ | mg $mg^{-1}$ | % |
| **MA555** | 11.1 ± 0.8 | 9.6 ± 0.4 | 9.6 ± 0.1 | 0.24 ± 0.02 | 0.36 ± 0.11 | 0.38 ± 0.03 | 0.1 ± 0.03 | Below Detection | Below Detection | 12.4 ± 1.1 |
| **MA564** | 35.6 ± 2.1 | 10.2 ± 0.9 | 8.5 ± 0.5 | 0.94 ± 0.12 | 1.34 ± 0.18 | 1.36 ± 0.04 | 0.11 ± 0.02 | 0.26 ± 0.06 | 0.28 ± 0.16 | 52.7 ± 6.1 |
| **CV** | 15 ± 2.1 | 8.6 ± 0.5 | 9.1 ± 0.1 | 0.36 ± 0.11 | 0.41 ± 0.15 | 0.39 ± 0.2 | 0.05 ± 0.02 | 0.1 ± 0.04 | 0.12 ± 0.08 | 17.1 ± 4.5 |
| **MH** | 16.2 ± 5.6 | 6.7 ± 1.1 | 6.9 ± 3.3 | 0.21 ± 0.19 | 0.28 ± 0.21 | 0.29 ± 0.18 | 0.09 ± 0.05 | 0.13 ± 0.09 | 0.15 ± 0.08 | 8.6 ± 3.4 |
| **MA (UK)**[‡] | - | - | 10 [‡] | - | - | 0.38 [‡] | - | - | 0.64[‡] | - |
| **CV (UK)** [‡] | - | - | 10.3 [‡] | - | - | 1.1 [‡] | - | - | 0.4 [‡] | - |

'-' indicates no data available, [‡] Data obtained or calculated from Henderson *et al.* [30], a – TOC for $AOM_c$ and $AOM_{1.5}$ and DOC for $AOM_{0.45}$